



## A Novel Direct Active and Reactive Power Control Method Using Fuzzy Super Twisting Algorithms and Modified Space Vector Modulation Technique for an Asynchronous Generator-based Dual-rotor Wind Powers

H. Benbouhenni\*

*Departement de Génie Electrique, Ecole Nationale Polytechnique d'Oran Maurice Audin, BP1523 EL M'NAOUER, Es-Sénia, Oran, Algérie*

### P A P E R I N F O

#### Paper history:

Received 13 April 2021

Accepted in revised form 16 May 2021

#### Keywords:

Asynchronous generator  
Direct active and reactive powers  
Dual-rotor wind power  
Fuzzy super-twisting sliding mode

### A B S T R A C T

This work presents a novel direct active and reactive powers command (DARPC) scheme based on fuzzy super twisting algorithms (FSTAs) of an asynchronous generator (ASG) integrated into dual-rotor wind power (DRWP) systems. The DRWP has two sets of blades. So it is more efficient for collecting power from wind in comparison to a traditional wind turbine. The scientific works indicate that a DRWP could extract additional 20-30% power compared to a traditional wind turbine. The conventional DARPC control scheme using the conventional integral-proportional (PI) regulators (DARPC-PI) has considerable reactive and active power oscillations. In order to guarantee an effective DARPC technique for the ASG-based DRWP system and minimize these oscillations, FSTAs are used in this work. Both DARPC strategies are presented and simulated from two tests using Matlab software. Simulation results showed the effectiveness of the designed DARPC control technique especially on the quality of the provided active and reactive power comparatively to the traditional DARPC control scheme with PI controllers.

doi: 10.5829/ijee.2021.12.02.02

### INTRODUCTION

DARPC or direct active and reactive powers command is a technique to control asynchronous generators (ASGs) by utilizing stator active and reactive powers. But the reactive and active power oscillations are occurred in the traditional DARPC strategy [1]. The principle of the DARPC strategy is detailed in literature [2–4]. In addition, DPC offers many advantages include: simplicity in calculations, robustness against ASG parameters, and fast dynamic response [5–7]. Although the DARPC strategy is getting more and more popular, it suffers from some drawbacks such as the large ripples of reactive and active powers. In order to overcome these disadvantages many researchers have been investigating on the DARPC strategy and they can be grouped under several headlines:

- Using artificial intelligence methods (Neural networks and fuzzy logic) on different sections of the system;

- Using different inverter topologies;
- Using sliding mode controller (SMC).

In this work, a novel fuzzy super-twisting algorithm (FSTA) and modified space vector modulation (MSVM) strategy has been designed to improve the stator active and reactive powers of the ASG on the DARPC technique.

The aim of this work is to improve the performance of the DARPC using FSTA controllers for ASG-based dual-rotor wind turbine (DRWT) system under variable speed wind and also to reduce fluctuations in reactive power, current, torque, and active power.

The FSTA method in the proposed technique rates active and reactive power errors and described the optimum space vector to reduce stator reactive and active power errors and oscillations. The simulation studies have been performed using Matlab logiciel board to effectiveness testing of the designed control strategy. In part II of this paper, the basic principles of the DARPC

\*Corresponding Author Email: [habib0264@gmail.com](mailto:habib0264@gmail.com)  
(H. Benbouhenni)

technique with PI controllers are presented. In part III, detailed information about the proposed strategy is introduced. Part IV gives the simulation results of the proposed technique. In conclusion, we provided a summary of the work performed.

### MATHEMATICAL MODELING OF DRWP SYSTEM

The DRWP system with ASG is shown in Figure 1. The DRWP consists of two wind powers. The mechanical power captured from the DRWP system is given by Benbouhenni [8]:

$$P_{DRWP} = P_{AT} + P_{MT} \quad (1)$$

where,  $P_{AT}$  is the mechanical power of auxiliary turbine, and  $P_{MT}$  is the mechanical power of auxiliary turbine.

The torque of DRWP is given by:

$$T_{DRWP} = T_{AT} + T_{MT} \quad (2)$$

where,  $T_{AT}$  is the torque of auxiliary turbine, and  $P_{MT}$  is the torque of auxiliary turbine.

Equations (3) and (4) represent the torque of the output main and auxiliary turbines [9].

$$T_{AT} = \frac{1}{2 \lambda_{AT}^3} \cdot \rho \cdot \pi \cdot R_{AT}^5 \cdot C_p \cdot \omega_{AT}^2 \quad (3)$$

$$T_{MT} = \frac{1}{2 \lambda_{MT}^3} \cdot \rho \cdot \pi \cdot R_{AT}^5 \cdot C_p \cdot \omega_{MT}^2 \quad (4)$$

where  $\lambda_{AT}$ ,  $\lambda_{MT}$ : the tip speed ration of the main and auxiliary turbines,  $R_{MT}$ ,  $R_{AT}$ : blade radius of the auxiliary and main turbines,  $\rho$ : the air density and  $\omega_{AT}$ ,  $\omega_{MT}$  the mechanical speed of the auxiliary and main turbines.

The tip speed ratios of the auxiliary and main turbines are given below:

$$\lambda_{AT} = \frac{\Omega_{AT} \cdot R_{AT}}{V_{AT}} \quad (5)$$

$$\lambda_{MT} = \frac{\Omega_{MT} \cdot R_{MT}}{V_{MT}} \quad (6)$$

where  $\Omega_{MT}$  is the rotational speed of the main rotor, and  $\Omega_{AT}$  is the rotational speed of the auxiliary rotor.

The power coefficient  $C_p$  equation is approximated using a non-linear function according to.

$$C_p(\lambda, \beta) = \frac{1}{\lambda + 0.08\beta} - \frac{0.035}{\beta^3 + 1} \quad (7)$$

where,  $\beta$  is pitch angle.

The wind speed on the main turbine is given below [10]:

$$V_x = V_1 \left( 1 - \frac{1 - \sqrt{(1 - C_T)}}{2} \left( 1 + \frac{2x}{\sqrt{1 + 4x^2}} \right) \right) \quad (8)$$

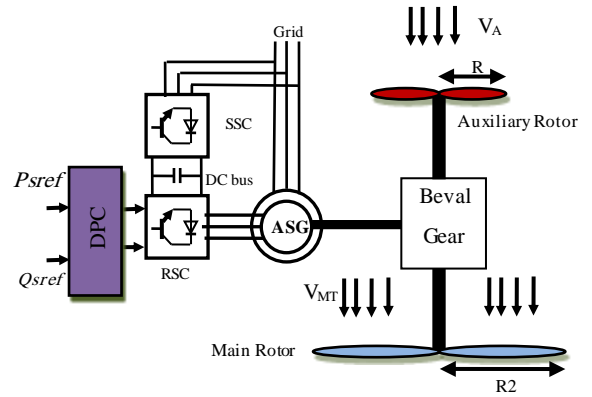


Figure 1. Structure of DRWP system with a ASG

with  $V_x$  is the velocity of the disturbed wind between rotors at point  $x$  and  $C_T$  the trust coefficient, which is taken to be 0.9;  $x$  the non-dimensional distance from the auxiliary rotor disk. So, with respect to  $x=15$ , the value of the  $V_x$  close to the main rotor is computable (rotors are located 15 meters apart from each other).

### MODIFIED SVM TECHNIQUE

The proposed SVM technique named as modified SVM (MSVM) technique is an effective modulation technique for uncertain inverter and it overcomes the main disadvantages of the traditional SVM strategy.

Figure 2 shows a block diagram representation of the MSVM technique approach for a two-level inverter in wind power. The principle of MSVM is detailed by Benbouhenni et al. [11]. This proposed strategy is based on calculation of the minimum and maximum of three-phase voltages. In this strategy, the sector and angle are not necessary to calculate. Modified SVM technique is used to minimize harmonic distortion (THD) in three-phase output current waveform compared to PWM technique.

The MSVM modulation technique is used to generate gate pulses to the IGBT switches of the ASG-based DRWP systems. The proposed MSVM technique is a simple algorithm compared to the classical SVM method and is more robust compared to the traditional PWM strategy. Benbouhenni et al. [12] proposed the use of an MSVM technique applied to the four-level inverter of ASG. The fuzzy MSVM technique is proposed to reduce the active and reactive powers [13]. The simulation results have shown the superiority of the two-level fuzzy MSVM strategy. Mehedi et al. [14], have proposed an MSVM to control the five-phase inverter and the results indicate that the proposed MSVM strategy-based technique is good at minimizing the torque undulation, THD value of stator current, and stator flux undulation.

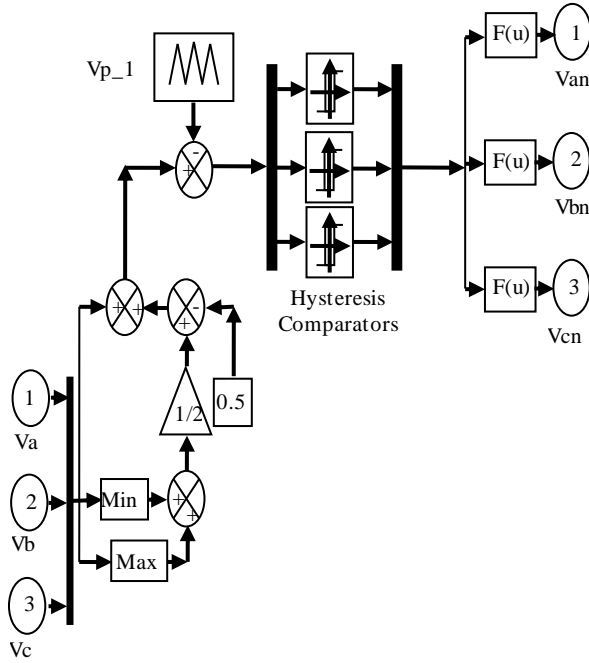


Figure 2. Modified SVM technique

**DARPC STRATEGY WITH PI CONTROLLERS**

In the DARPC-PI technique, the control of an ASG involves the direct command of the active and reactive powers by using two PI regulators [15]. This technique is a robust, easy, and simple technique. Stator active and reactive powers are estimated using Equations (9) and (10) [16].

$$P_s = -\frac{3}{2} \frac{L_m}{\sigma \cdot L_s \cdot L_r} \cdot (V_s \cdot \psi_{r\beta}) \tag{9}$$

$$Q_s = -\frac{3}{2} \left( \frac{V_s}{\sigma \cdot L_s} \cdot \psi_{r\beta} - \frac{V_s \cdot L_m}{\sigma \cdot L_s \cdot L_r} \cdot \psi_{r\alpha} \right) \tag{10}$$

while,

$$\sigma = 1 - \frac{M^2}{L_r L_s} \tag{11}$$

These estimated values are compared to reference values and the resultant errors are applied to the PI regulators. Two PI controllers, as reactive and active PI regulators, generate other command parameters on the DARPC-MSVM technique or (DARPC-PI). The basic schematic representation of the DARPC-PI technique for ASG is shown in Figure 3.

The rotor flux can be estimated by:

$$\begin{cases} \psi_{r\alpha} = \int (v_{r\alpha} - R_r i_{r\alpha}) dt \\ \psi_{r\beta} = \int (v_{r\beta} - R_r i_{r\beta}) dt \end{cases} \tag{12}$$

The rotor flux amplitude is given by:

$$\psi_r = \sqrt{\psi_{r\alpha}^2 + \psi_{r\beta}^2} \tag{13}$$

where:

$$|\psi_r| = \frac{V_r}{w_r} \tag{14}$$

The reactive and active PI regulators gains (Ki and Kp) were found after performing simulations in Matlab logiciel. The gianses of PI regulator is stated in Table 1.

**THE FSTA METHOD BASED DARPC METHOD**

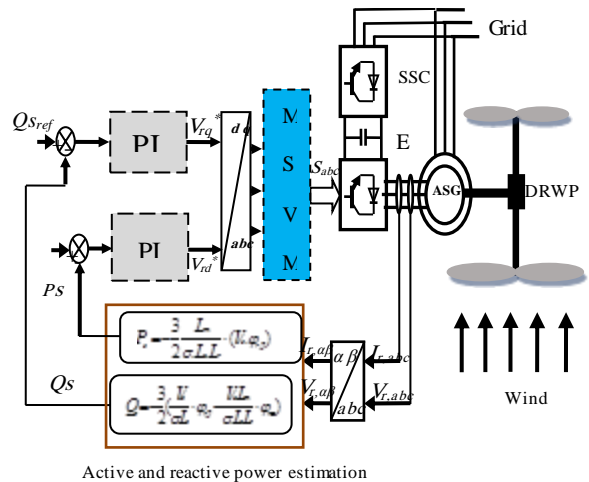
The DARPC scheme with PI controllers (DARPC-PI) offers some drawbacks associated with the large active and reactive powers ripples. In order to reduce these ripples, an STA technique with a fuzzy controller (FC) was designed. The origin of the DARPC-FSTA method is like to the DARPC-PI technique. The difference is using an FSTA algorithm to replace the conventional PI controllers. Also, the FLC is not dependent on the accurate mathematical model of the system [17]. It is based on ‘IF...THEN’ rules and experiences of human beings. In this work, using the advantage of FLC and STA, a DARPC method is presented.

**A. Design of PI controller based on STA algorithm**

The STA algorithm is based on the design of the discontinuous command signal that drives the system states toward special surfaces in state space [18]. Two

Table 1. PI regulator gains

<b>Ki</b>	0.6
<b>Kp</b>	0.00005



Active and reactive power estimation

Figure 3. DARPC-PI technique

STA algorithms are selected for stator reactive and active power command. On the other hand, the STA algorithm is one of the robust techniques [19]. It is a particular operation mode of variable structure control systems. These techniques were used in numerous research works in the past years [20–24]. In the ASG command using the STA algorithm, the manifolds are chosen according to the error between the measured signals and the reference input signal. Considering that  $e_1$  and  $e_2$  are the errors of the stator active and the reactive power, we have the following:

$$\begin{bmatrix} e_1 \\ e_2 \end{bmatrix} = \begin{bmatrix} P_{sref} - P_s \\ Q_{sref} - Q_s \end{bmatrix} \quad (15)$$

The expression of the manifolds has the following form.

$$\begin{bmatrix} S(P_s) \\ S(Q_s) \end{bmatrix} = \begin{bmatrix} P_{sref} - P_s \\ Q_{sref} - Q_s \end{bmatrix} \quad (16)$$

The STA algorithms active and reactive power controllers are designed to respectively change the  $q$  and  $d$ -axis voltages as in Equations (17) and (18) [11].

$$\begin{cases} V_{dr} = K_1 |S_{Q_r}|^r \text{sign}(S_{Q_r}) + V_{dr1} \\ \dot{V}_{dr1} = K_2 \text{sign}(S_{Q_r}) \end{cases} \quad (17)$$

$$\begin{cases} V_{qr} = K_1 |S_{T_{em}}|^r \text{sign}(S_{T_{em}}) + V_{qr1} \\ \frac{dV_{qr1}}{dt} = K_2 \text{sign}(S_{T_{em}}) \end{cases} \quad (18)$$

where, the constant gains  $k_1$  and  $k_2$  must check the stability conditions.

Figure 4 shows the block diagram of STA algorithms of active and reactive powers.

**B. Designe of FLC based on STA algorithm**

FSTA algorithm is a merge between the STA algorithm and FLC technique, where the switching term,  $\text{Sign}(S(x))$ , has been replaced by the FLC technique. The proposal of an STA algorithm incorporating the FLC method helps in achieving minimized active and reactive powers oscillations, easy method, simple technique, and robust technique compared to vector command method. The proposed FSTA algorithm, which is proposed to command the active and reactive powers of the ASG is shown in Figure 5. The fuzzy sets have been defined as follows: NB: Negative Big, NM: Negative Middle, NS: Negative Small, PS: Positive Small, PB: Positive Big, EZ: Equal Zero, and PM: Positive Middle. Membership functions in triangular shape are shown in Figures 6 and 7, respectively. Table 2 shows the proposed rule bases for the FSTA algorithms [25, 26].

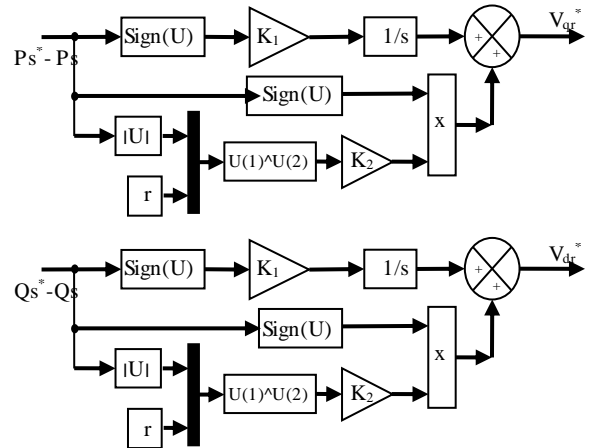


Figure 4. Block diagram of STA technique

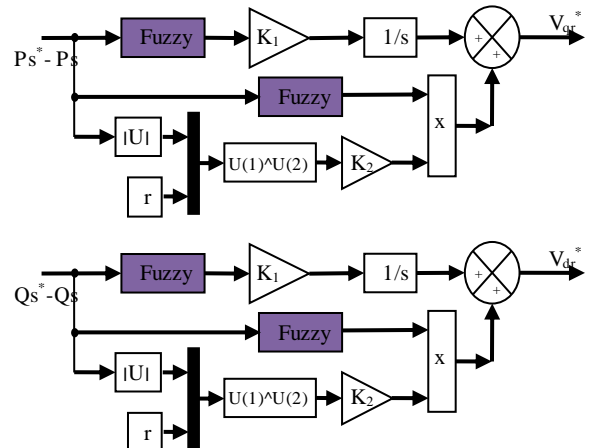


Figure 5. Block diagram of FSTA technique

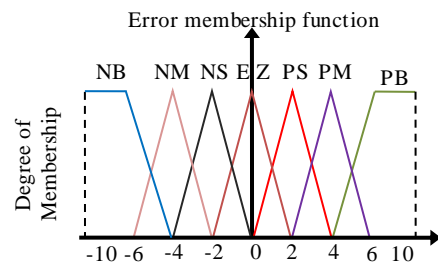


Figure 6. Membership functions for sliding surface

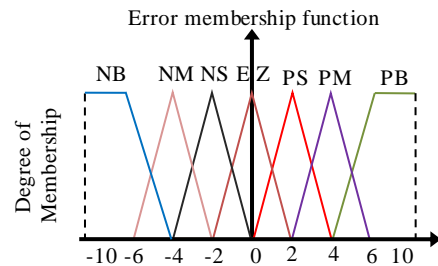


Figure 7. Membership functions for output variables

**Table 2.** FSTA algorithm rule bases

e	NB	NM	NS	EZ	PS	PM	PB
Δe							
NS	NB	NB	NM	NS	EZ	PS	PM
NM	NB	NB	NB	NM	NS	EZ	PS
NB	NB	NB	NB	NB	NM	NS	EZ
PS	NM	NS	EZ	PS	PM	PB	PB
EZ	NB	NM	NS	EZ	PS	PM	PB
PB	EZ	PS	PM	PB	PB	PB	PB
PM	NS	EZ	PS	PM	PB	PB	PB

The proprieties of our regulators are given in the Table 3.

The structure of the DARPC technique with the FSTA algorithms applied to the ASG-DRWP is illustrated in Figure 8.

**SIMULATION RESULTS**

To study the effectiveness of the designed DARPC DARPC-PI and DARPC-FSTA technique, the simulation of the system was accomplished using Matlab logiciel and

**Table 3.** Proprieties of the FLC technique

<b>Fis type</b>	Mamdani
<b>And method</b>	Min
<b>Or method</b>	Max
<b>Implication</b>	Min
<b>Aggregation</b>	Max
<b>Defuzzification</b>	Centroid

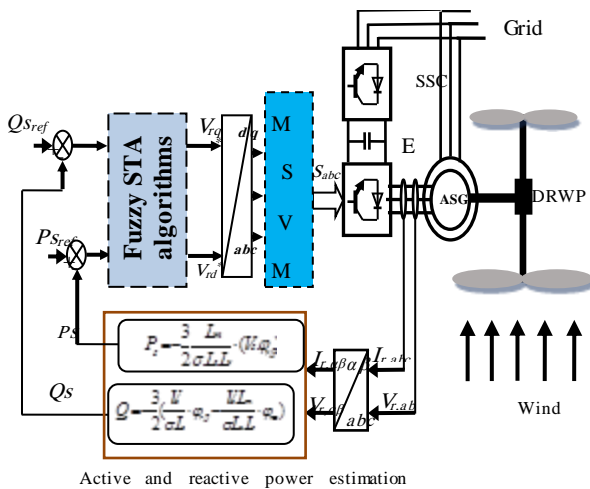


**Figure 8.** Block diagram of DARPC-FSTA control

fuzzy logic Toolbox. The DFIG used in this case study is a 1,5MW, 380/690V, 50Hz, two poles, with the following parameters:  $R_s= 0.012\Omega$ ,  $L_r=0.0136 H$ ,  $M= 0.0135 H$ ,  $R_r= 0.021\Omega$ ,  $L_s=0.0137 H$  [27].

The ASG has the following mechanical parameters:  $J = 1000 \text{ Kg.m}^2$ ,  $f_r= 0.0024 \text{ Nm/s}$ .

From the simulation results are presented in Figures 9 and 10. It is apparent that the THD value of current for the DARPC-FSTA strategy is reduced (see Table 4).

From the system responses given in Figures 11 and 12 for DARPC-PI and DARPC-FSTA technique the stator active and reactive power tracks the reference powers without overshoot, with zero steady-state error. Figure 13 shows the torque of both techniques. Note that torque is related to active power.

From Figure 14 can be seen that the amplitudes of the stator phase currents depend on the state of the drive system and the value of the load active power.

The zoom in the active power, torque, and stator current are shown in Figures 15, 16 and 17, respectively. It can be seen that the DARPC control with FSTA algorithms minimized the undulations in active power, torque, and current compared to the DARPC strategy with PI controllers.

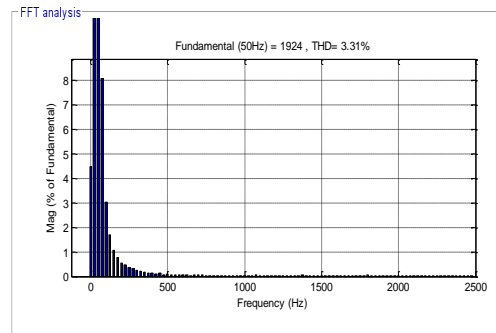


**Figure 9.** THD value of the current (DARPC-PI)

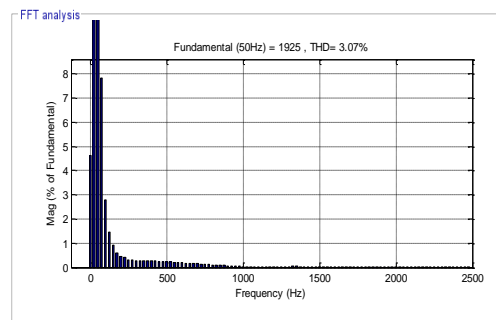


**Figure 10.** THD value of the current (DARPC-FSTA)

**Table 4.** THD value of both techniques

<b>DARPC-PI</b>	3.31%
<b>DARPC-FSTA</b>	3.07%

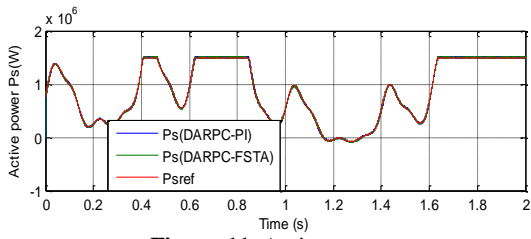


Figure 11. Active power

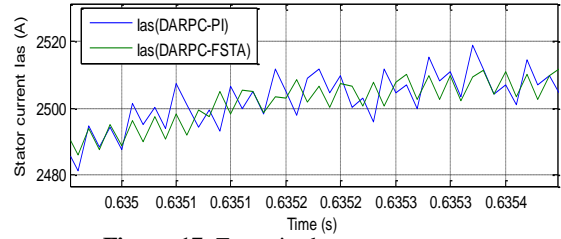


Figure 17. Zoom in the stator current

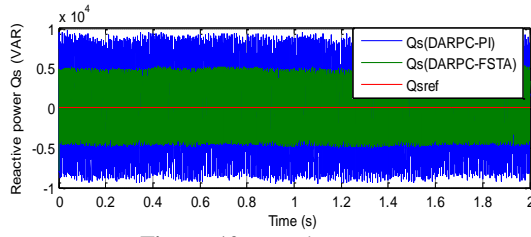


Figure 12. Reactive power

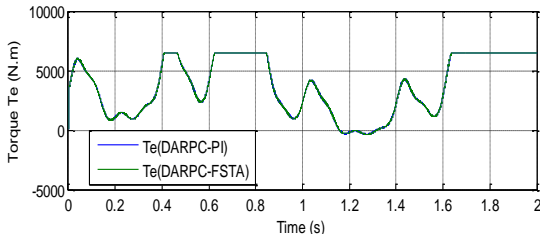


Figure 13. Electromagnetic torque

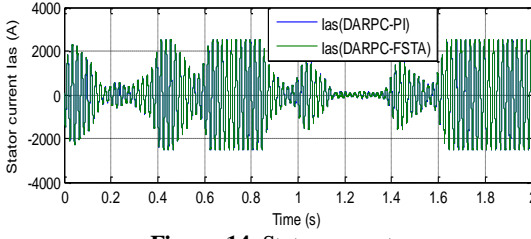


Figure 14. Stator current

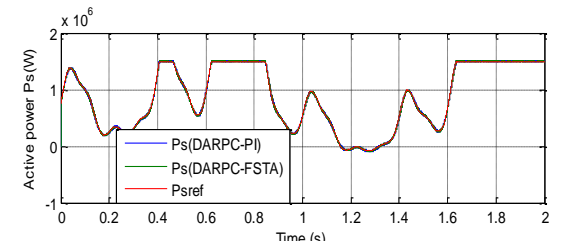


Figure 18. Active power

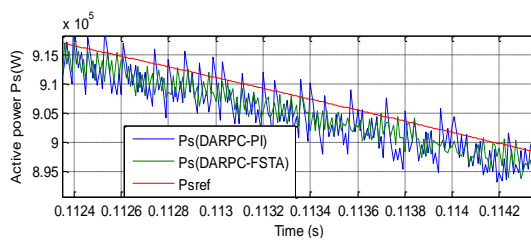


Figure 15. Zoom in the active power

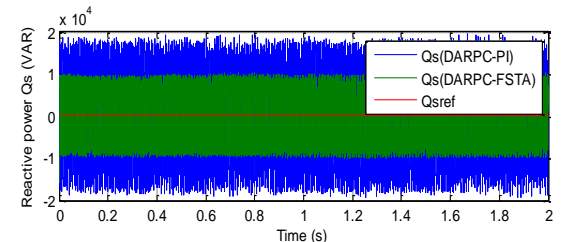


Figure 19. Reactive power

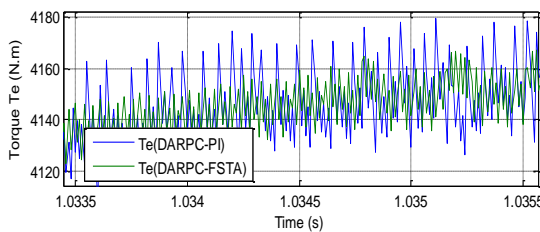


Figure 16. Zoom in the torque

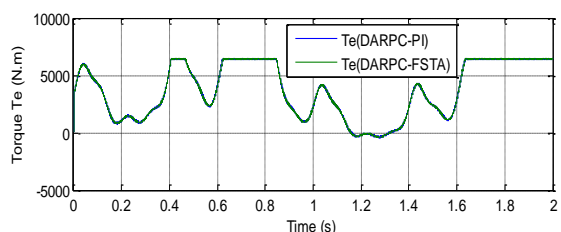


Figure 20. Torque

**Robustness test (RT)**

In this test, the nominal value of the  $R_r$  and  $R_s$  is multiplied by 2, the values of inductances  $L_s$ ,  $M$ , and  $L_r$  are multiplied by 0.5. Simulation results are presented in Figures 18-23. As it's shown by these figures, these variations present an apparent effect on the torque, current, active and reactive power curves, and that the effect appears more significant for the DARPC using PI controllers compared to DARPC using FSTA algorithms (See Figures. 24-26).

The THD value of the current in the DARPC using the FSTA algorithms has been minimized significantly (See Figures 22 and 23). Table 5 shows the THD value of both strategies. Thus it can be concluded that the proposed DARPC using FSTA algorithms is more robust than the DARPC using the PI controllers.

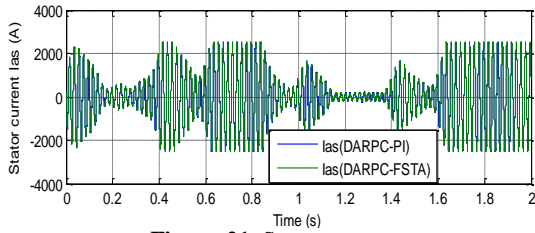


Figure 21. Stator current

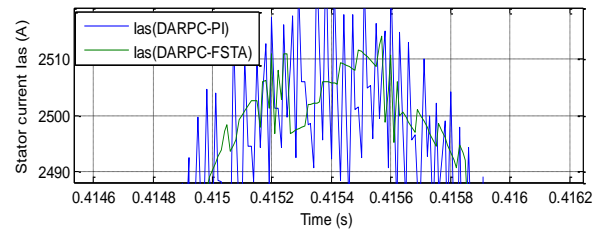


Figure 26. Zoom in the stator current

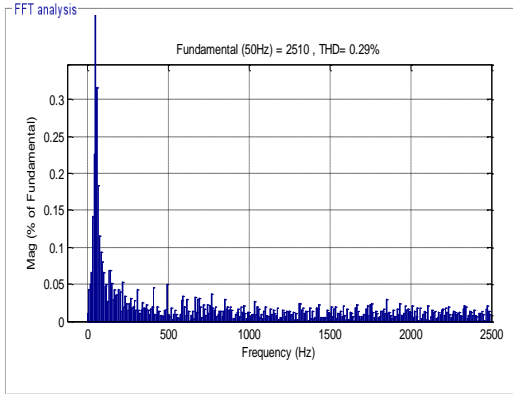


Figure 22. THD value of the current (DARPC-PI)

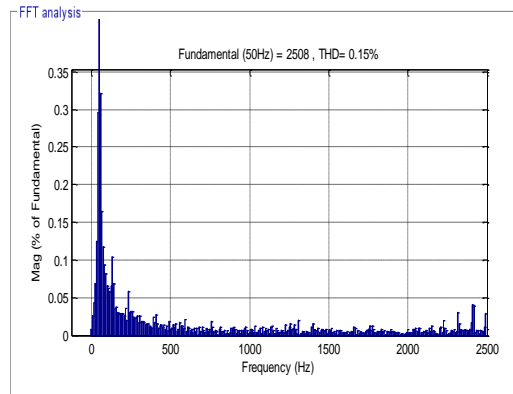


Figure 23. THD value of the current (DARPC-FSTA)

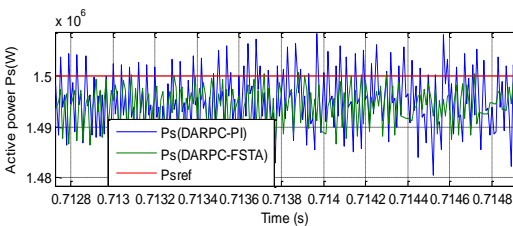


Figure 24. Zoom in the active power

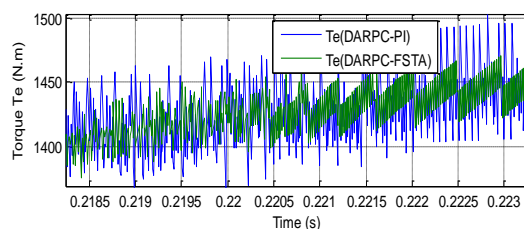


Figure 25. Zoom in the torque

On the other hand, this designed technique reduced the THD value of current compared to other techniques (see Table 5). Based on the results above, it can be said that the DARPC-FSTA control technique has proven its efficiency in reducing ripples and chattering phenomena in addition to keeping the same advantages of the traditional DARPC method.

Table 5. Compare results with other methods

Ref.	Method Name	THD (%)
[22]	Second Order Continuous Sliding Mode – Direct Torque Control SOCSM-DTC	0.98
[27]	Direct Power Control DPC	4.88
[28]	Virtual-Flux Direct Power Control VFDP	4.19
[29]	Sliding Mode Control SMC	3.05
	Field Oriented Control FOC	3.7
Proposed techniques	DARPC-PI	0.29
	DARPC-FSTA	0.15

## CONCLUSION

In this work, a robust strategy is designed to improve the effectiveness of the DARPC-PI for the ASG-based DRWP systems. FSTA technique is proposed to replace the classical PI controllers of the DARPC-PI control scheme. The proposed strategy preserves the advantages of the traditional DARPC such as less parameter dependence and simplicity. The effectiveness of DARPC-PI and designed strategy is studied under, THD value of current and powers oscillations. By comparing the performances of the designed strategy with conventional DARPC-PI, it can be concluded that the designed strategy has minimized the THD value of current. The proposed strategy has been very successful in improving the energy quality provided by the wind generator.

## REFERENCES

- Amrane, F., and Chaiba, A. 2016. "A novel direct power control for grid-connected doubly fed induction generator based on hybrid artificial intelligent control with space vector modulation." *Revue*

- Roumaine des Sciences Techniques. Série Électrotechnique et Énergétique*, 61(3), pp.263–268. Retrieved from <http://dspace.univ-setif.dz:8888/jspui/handle/123456789/2585>
2. Shehata, E. G., and Salama, G. M. 2013. "Direct power control of DFIGs based wind energy generation systems under distorted grid voltage conditions." *International Journal of Electrical Power and Energy Systems*, 53, pp.956–966. <https://doi.org/10.1016/j.ijepes.2013.06.006>
  3. Jou, S.-T., Lee, S.-B., Park, Y.-B., and Lee, K.-B. 2009. "Direct Power Control of a DFIG in Wind Turbines to Improve Dynamic Responses." *Journal of Power Electronics*, 9(5), pp.781–790. Retrieved from <https://www.koreascience.or.kr/article/JAKO200931559974840.pdf>
  4. Wu, Y. K., and Yang, W. H. 2016. "Different Control Strategies on the Rotor Side Converter in DFIG-based Wind Turbines." *Energy Procedia*, 100, pp. 551–555. <https://doi.org/10.1016/j.egypro.2016.10.217>
  5. Heydari, E., Rafiee, M., and Pichan, M. 2018. "Fuzzy-genetic algorithm-based direct power control strategy for DFIG." *Iranian Journal of Electrical and Electronic Engineering*, 14(4), pp.353–361. <https://doi.org/10.22068/IJEEE.14.4.353>
  6. Izanlo, A., Kazemi, M. V., and Asghar Gholamian, S. 2018. "Comparative study between two sensorless methods for direct power control of doubly fed induction generator." *Revue Roumaine des Sciences Techniques. Série Électrotechnique et Énergétique*, 62, pp.358–364. Retrieved from <https://www.researchgate.net/publication/322364899>
  7. Shehata, E. G. 2015. "Sliding mode direct power control of RSC for DFIGs driven by variable speed wind turbines." *Alexandria Engineering Journal*, 54(4), pp.1067–1075. <https://doi.org/10.1016/j.aej.2015.06.006>
  8. Benbouhenni, H. 2021. "Intelligent super twisting high order sliding mode controller of dual-rotor wind power systems with direct attack based on doubly-fed induction generators." *Journal of Electrical Engineering, Electronics, Control and Computer Science*, 7(4), pp.1–8. Retrieved from <https://jeeccs.net/index.php/journal/article/view/219>
  9. Yahdou, A., Djilali, A. B., Boudjema, Z., and Mehedi, F. 2020. "Improved Vector Control of a Counter-Rotating Wind Turbine System Using Adaptive Backstepping Sliding Mode." *Journal Européen des Systèmes Automatisés*, 53(5), pp.645–651. <https://doi.org/10.18280/jesa.530507>
  10. Yahdou, A., Hemici, B., and Boujema, Z. 2015. "Sliding mode control of dual rotor wind turbine system." *he Mediterranean Journal of Measurement and Control*, 11(2), pp.412–419. Retrieved from [https://scholar.google.com/scholar?hl=en&as\\_sdt=0%2C5&q=Sliding+mode+control+of+dual+rotor+wind+turbine+system&btnG=](https://scholar.google.com/scholar?hl=en&as_sdt=0%2C5&q=Sliding+mode+control+of+dual+rotor+wind+turbine+system&btnG=)
  11. Benbouhenni, H., Boudjema, Z., and Belaidi, A. 2020. "Direct power control with nstsm algorithm for dfig using svpwm technique." *Iranian Journal of Electrical and Electronic Engineering*, 17(1), pp.1–11. <https://doi.org/10.22068/IJEEE.17.1.1518>
  12. Benbouhenni, H., Boudjema, Z., and Belaidi, A. 2019. "Using four-level NSVM technique to improve DVC control of a DFIG based wind turbine systems." *Periodica polytechnica Electrical engineering and computer science*, 63(3), pp.144–150. <https://doi.org/10.3311/PPee.13636>
  13. Benbouhenni, H., Boudjema, Z., and Belaidi, A. 2018. "Indirect Vector Control of a DFIG Supplied by a Two-level FSVM Inverter for Wind Turbine System." *Majlesi Journal of Electrical Engineering*, 13(1), pp.45–54. Retrieved from <http://mjee.iaumajlesi.ac.ir/index/index.php/ee/article/view/2693>
  14. Mehedi, F., Yahdou, A., Djilali, A., and Benbouhenni, H. 2020. "Direct Torque Fuzzy Controlled Drive for Multi-phase IPMSM Based on SVM Technique." *Journal Européen des Systèmes Automatisés*, 53(2), pp.259–266. <https://doi.org/10.18280/jesa.530213>
  15. Massoum, S., Meroufel, A., Massoum, A., and Wira, P. 2017. "A direct power control of the doubly-fed induction generator based on the SVM Strategy." *Elektrotehniski Vestnik*, 84(5), pp.235–240. Retrieved from <https://ev.fe.uni-lj.si/5-2017/Massoum.pdf>
  16. Djeriri, Y., Meroufel, A., Massoum, A., and Boudjema, Z. 2014. "A comparative study between field oriented control strategy and direct power control strategy for DFIG." *Journal of Electrical Engineering*, 14(2), pp.1–9. Retrieved from <http://new.jee.ro/index.php/jee/article/view/WC1374511392W51e6d1206e644>
  17. Chabni, F., Taleb, R., Benbouali, A., and Bouthiba, M. A. 2016. "The Application of Fuzzy Control in Water Tank Level Using Arduino." (*IJACSA International Journal of Advanced Computer Science and Applications*, 7(4), pp.261–265. Retrieved from <https://pdfs.semanticscholar.org/82f2/9592c049b1d5803173025fcbca24627bb1bb.pdf>
  18. Benbouhenni, H., Boudjema, Z., and Belaidi, A. 2018. "Neuro-second order sliding mode control of a DFIG supplied by a two-level NSVM inverter for wind turbine system." *Iranian Journal of Electrical and Electronic Engineering*, 14(4), pp.362–373. <https://doi.org/10.22068/IJEEE.14.4.362>
  19. Benbouhenni, H. 2018. "Fuzzy Second Order Sliding Mode Controller Based on Three-Level Fuzzy Space Vector Modulation of a DFIG for Wind Energy Conversion Systems." *Majlesi Journal of Mechatronic Systems*, 7(3), pp.17–26. Retrieved from <http://journals.iaumajlesi.ac.ir/ms/index/index.php/ms/article/view/369>
  20. Yahdou, A., Boudjema, Z., Hemici, B., and Boudjema, Z. 2016. "Second order sliding mode control of a dual-rotor wind turbine system by employing a matrix converter." *Journal of Electrical Engineering*, pp.1–11. Retrieved from <https://www.researchgate.net/publication/317216127>
  21. El, S. A., Ardjoum, M., and Abid, M. 2015. "Fuzzy sliding mode control applied to a doubly fed induction generator for wind turbines." *Turkish Journal of Electrical Engineering & Computer Sciences*, 23(6), pp.1673–1686. <https://doi.org/10.3906/elk-1404-64>
  22. Boudjema, Z., Taleb, R., Djeriri, Y., and Yahdou, A. 2017. "A novel direct torque control using second order continuous sliding mode of a doubly fed induction generator for a wind energy conversion system." *Turkish Journal of Electrical Engineering & Computer Sciences*, 25(2), pp.965–975. <https://doi.org/10.3906/elk-1510-89>
  23. Benbouhenni, H. 2018. "Neuro-sconde order sliding mode field oriented control for DFIG based wind turbine." *International Journal of Smart Grid*, 2(4), pp.209–217. Retrieved from <https://www.academia.edu/download/58084192/25-144-1-PB.pdf>
  24. Bouyekni, A., Taleb, R., Boudjema, Z., and Kahal, H. 2018. "A second-order continuous sliding mode based on DPC for wind-turbine-driven DFIG." *Elektrotehniski Vestnik*, 85(2), pp.29–36. Retrieved from <https://ev.fe.uni-lj.si/1-2-2018/Bouyekni.pdf>
  25. Benbouhenni, H., Boudjema, Z., and Belaidi, A. 2018. "DFIG-based WT system using FPWM inverter." *International Journal of Smart Grid-ijSmartGrid*, 2(3), pp.142–154. Retrieved from <https://www.ijsmartgrid.com/index.php/ijsmartgridnew/article/view/16>
  26. Benbouhenni, H. 2018. Comparative Study Between NSVM and FSVM Strategy for a DFIG-based Wind Turbine System Controlled by Neuro-Second Order Sliding Mode. *Majlesi Journal of Mechatronic Systems*, 7(1), pp.33–43. Retrieved from <https://iranjournals.nlai.ir/handle/123456789/712266>
  27. Mohd Yusoff, N. A., M. Razali, A., Abdul Karim, K., Sutikno, T., and Jidin, A. 2017. "A Concept of Virtual-Flux Direct Power Control of Three-Phase AC-DC Converter." *International Journal*



- of *Power Electronics and Drive Systems (JPEDS)*, 8(4), pp.1776-1784. <https://doi.org/10.11591/ijpeds.v8.i4.pp1776-1784>
28. Boudjema, Z., Meroufel, A., Djeriri, Y., Boudjema, Z., Meroufel, A., Djerriri, Y., and Bounadja, E. 2013. "Fuzzy sliding mode control of a doubly fed induction generator for wind energy conversion." *Carpathian Journal of Electronic and Computer Engineering*, 6(2), pp.7-14. Retrieved from <http://cjece.ubm.ro/vol/6-2013/202-6117.pdf>
29. Amrane, F., Chaiba, A., Eddine Babes, B., and Mekhilef, S. 2016. "Design and implementation of high performance field oriented control for grid-connected doubly fed induction generator via hysteresis rotor current controller." *Revue Roumaine des Sciences Techniques. Série Électrotechnique et Énergétique*, 61(4), pp.319-324. Retrieved from [http://revue.elth.pub.ro/upload/66838802\\_FAmrane\\_RRST\\_4\\_2016\\_pp\\_319-324.pdf](http://revue.elth.pub.ro/upload/66838802_FAmrane_RRST_4_2016_pp_319-324.pdf)

#### COPYRIGHTS

©2021 The author(s). This is an open access article distributed under the terms of the Creative Commons Attribution (CC BY 4.0), which permits unrestricted use, distribution, and reproduction in any medium, as long as the original authors and source are cited. No permission is required from the authors or the publishers.



#### Persian Abstract

#### چکیده

این کار یک طرح جدید قدرت مستقیم و راکتیو فرمان (DARPC) مبتنی بر الگوریتم‌های پیچش فوق‌العاده فازی (FSTA) یک ژنراتور ناهمزمان (ASG) یکپارچه شده در سیستم‌های قدرت باد دو روتور (DRWP) را ارائه می‌دهد. DRWP دارای دو مجموعه تیغه است. بنابراین در مقایسه با یک توربین بادی سنتی برای جمع‌آوری انرژی از باد کارآمدتر است. کارهای علمی نشان می‌دهد که یک DRWP می‌تواند در مقایسه با یک توربین بادی سنتی ۲۰-۳۰ درصد انرژی اضافی استخراج کند. طرح کنترل DARPC متداول با استفاده از تنظیم‌کننده‌های متناوب متناسب با انتگرال (DARPC-PI) دارای نوسانات توان واکنش‌پذیر و فعال قابل توجهی است. به منظور تضمین روش موثر DARPC برای سیستم DRWP مبتنی بر ASG و به حداقل رساندن این نوسانات، از FSTA در این کار استفاده می‌شود. هر دو استراتژی DARPC با استفاده از نرم‌افزار Matlab از دو آزمون ارائه و شبیه‌سازی شده‌اند. نتایج شبیه‌سازی اثر بخشی روش کنترل DARPC طراحی شده به ویژه بر کیفیت توان فعال و راکتیو ارائه شده را نسبتاً به طرح کنترل سنتی DARPC با کنترل‌کننده‌های PI نشان می‌دهد.